Journal of Biomolecular NMR, **16:** 303–312, 2000.
KLUWER/ESCOM

Solution structure of the human BTK SH3 domain complexed with a proline-rich peptide from p120^{cbl}

Shiou-Ru Tzeng, Yuan-Chao Lou, Ming-Tao Pai, Moti L. Jain & Jya-Wei Cheng*
Division of Structural Biology and Biomedical Science, Department of Life Science, National Tsing Hua University, Hsinchu 300, Taiwan

Received 28 September 1999; Accepted 24 January 2000

Key words: BTK, peptide binding, proline-rich peptide, SH3 domain, XLA

Abstract

X-linked agammaglobulinemia (XLA), an inherited disease, is caused by mutations in the Bruton's tyrosine kinase (BTK). The absence of functional BTK leads to failure of B cell differentiation which incapacitates antibody production in XLA patients leading to, sometimes lethal, bacterial infections. Point mutation in the BTK gene that leads to deletion of C-terminal 14 aa residues of BTK SH3 domain was found in one patient family. To understand the role of BTK in B cell development, we have determined the solution structure of BTK SH3 domain complexed with a proline-rich peptide from the protein product of c-cbl protooncogene (p120^{cbl}). Like other SH3 domains, BTK SH3 domain consists of five β-strands packed in two β-sheets forming a β-barrel-like structure. The rmsd calculated from the averaged coordinates for the BTK SH3 domain residues 218–271 and the p120^{cbl} peptide residues 6–12 of the complex was 0.87 Å (±0.16 Å) for the backbone heavy atoms (N, C, and C_α) and 1.64 Å (±0.16 Å) for all heavy atoms. Based on chemical shift changes and inter-molecular NOEs, we have found that the residues located in the RT loop, n-Src loop and helix-like loop between β4 and β5 of BTK SH3 domain are involved in ligand binding. We have also determined that the proline-rich peptide from p120^{cbl} binds to BTK SH3 domain in a class I orientation. These results correlate well with our earlier observation that the truncated BTK SH3 domain (deletion of β4, β5 and the helix-like loop) exhibits weaker affinity for the p120^{cbl} peptide. It is likely that the truncated SH3 domain fails to present to the ligand the crucial residues in the correct context and hence the weaker binding. These results delineate the importance of the C-terminus in the binding of SH3 domains and also indicate that improper folding and the altered binding behavior of mutant BTK SH3 domain likely lead to XLA.

Introduction

X-linked agammaglobulinemia (XLA) patients show markedly reduced or absence of serum immunoglobulins of all isotypes and fail to produce antigen-specific antibodies, making them unusually susceptible to pyrogenic bacterial infection and enteroviral diseases (Zhu et al., 1994). This gene defect is intrinsic to B cell lineage: T-cell dependent immunity is normal in XLA patients (Tsukada et al., 1993). The number of pre-B cells in the patient's bone marrow is normal; the defect thus resides in the development pathway of B cells (Tsukada et al., 1993; Smith et al., 1994a, b). The gene responsible for this disease encodes a cytoplasmic tyrosine kinase, Bruton's tyrosine kinase (BTK) (Vetrie et al., 1993). This kinase is expressed in early and mature human B cell lines but is absent in terminally differentiated plasma cell lines. This distribution indicates that BTK, like other non-receptor tyrosine kinases, is required for normal B cell differentiation. Mutations or deletions in the BTK gene were detected in unrelated XLA patients (Hammarstrom et al., 1993; Smith et al., 1994b), suggesting strongly that the kinase is directly involved in the process of B cell development.

BTK, along with Tec, Itk and Bmx, belongs to a small family of tyrosine kinases (the Tec family)

*To whom correspondence should be addressed. E-mail: lscjw@life.nthu.edu.tw

that share common structural features (Vetrie et al., 1993; Pawson, 1995; Shokat, 1995). Like many other cytoplasmic tyrosine kinases involved in signaling pathways, BTK contains an N-terminal pleckstrin homology (PH) domain, a proline-rich Tec homology (TH) domain, a Src homology 2 (SH2) domain, a Src homology 3 (SH3) domain and a catalytic tyrosine kinase domain (Figure 1A) (Yu and Schreiber, 1994; Cohen et al., 1995; Pawson, 1995; Shokat, 1995; Sudol, 1998).

The SH3 and SH2 domains are small protein modules that mediate protein–protein interactions and occur in many proteins involved in intracellular signal transduction (Yu and Schreiber, 1994; Cohen et al., 1995; Pawson, 1995; Shokat, 1995; Sudol, 1998). SH3 domains bind to proline-rich sequences and SH2 domains bind to phosphotyrosine sequences of the receptor protein tyrosine kinases (Kuriyan and Cowburn, 1993; Pawson and Schlessinger, 1993; Songyang et al., 1993). The structural basis for interaction between peptide ligands and SH3 domains is now well understood (Feng et al., 1994; Lim et al., 1994). Two classes, class I and II, are defined according to their mode of binding. Ligands of both the classes contain a PXXP core sequence that anchors the ligand to the receptor in the polyproline type II (PPII) helical conformation, whereas the nearby flanking sequences provide a binding specificity (Wu et al., 1995). Although the core sequences of the ligands which can bind to different SH3 domains are conserved, the flanking sequences are unique to individual SH3 domains and bind to a specific pocket (Alexandropoulos et al., 1995; Feng et al., 1995; Sparks et al., 1996).

Recently, the solution structure of free BTK SH3 domain was reported (Hansson et al., 1998). The BTK SH3 domain shows the typical SH3 topology, forming mainly a β-barrel type structure. However, little is known about its interaction with proline-rich peptides. The BTK SH3 domain has been shown to bind with the protein product of c-cbl protooncogene ($p120^{cbl}$) (Cory et al., 1995). Previously, we quantitated the affinity of BTK SH3 domain with proline-rich peptides from $p120^{cbl}$ and from its own TH domain (Patel et al., 1997). The point mutation resulting in the deletion of 14 amino acids constituting the C-terminus of BTK SH3 domain (residues 260–273) has been identified as a cause of XLA in one patient family (Zhu et al., 1994). We found that the association of the truncated SH3 domain with proline-rich peptides was weaker than with intact SH3 domain (Patel et al., 1997). We have also demonstrated earlier that the mutation (loss of the C-terminal 14 aa residues) results in transformation of the β-barrel structure of BTK SH3 domain to random coil conformation (Chen et al., 1996). Therefore, the mutation-truncation that causes XLA snaps the SH3 domain of its ability to bind to its target, probably due to the aberrant folding. The altered binding behavior likely renders the kinase abnormal. The structural study of the association of various domains with their ligands can help to define consensus motifs and their modes of binding. This may lead to the foundation for the design of peptide inhibitors of proteins that block their interaction with other proteins. Besides, it would also provide more insight into the control of signaling processes. In this paper we report the solution structure of BTK SH3 domain complexed with a proline-rich peptide from $p120^{cbl}$ which provides a molecular basis for understanding the role of BTK in B cell development.

Materials and methods

Protein preparation and purification

The DNA fragments encoding residues 216–273 of human BTK were amplified by PCR. The amplified PCR products were subcloned into pET-21b vector. Plasmids encoding BTK SH3 domain were introduced into *E. coli* strains BL21(DE3), and transformants were cultured overnight at 37 °C in SOB medium supplemented with ampicilin (100 μg/ml). ^{15}N-labeled samples were expressed in cells grown in M9 minimal media containing 1 g/L $^{15}NH_4Cl$ and 2 g/L glucose. The cell lysates were centrifuged and supernatant from the centrifugation was applied to an ionic Q column (Pharmacia) at 4 °C. The samples were then eluted with a 50 to 500 mM NaCl gradient in a 20 mM Tris buffer at pH 8.0. Fractions containing BTK-SH3 were pooled, concentrated, and added to a 1.6 cm × 60.0 cm Sephacryl S-100 column (Pharmacia). Finally the protein was eluted with NMR buffer containing 50 mM K_2HPO_4 (pH 6.5), 100 mM NaCl, 10 mM NaN_3, and 0.1 mM EDTA. The final protein concentration for NMR study was 2 mM in 90% H_2O/10% D_2O.

Peptide synthesis

The peptide SLHKDKPLPVPPYQ was synthesized on an Applied Biosystems 431A peptide synthesizer using standard solid phase methods. After synthesis, the peptide was deprotected at side chains and

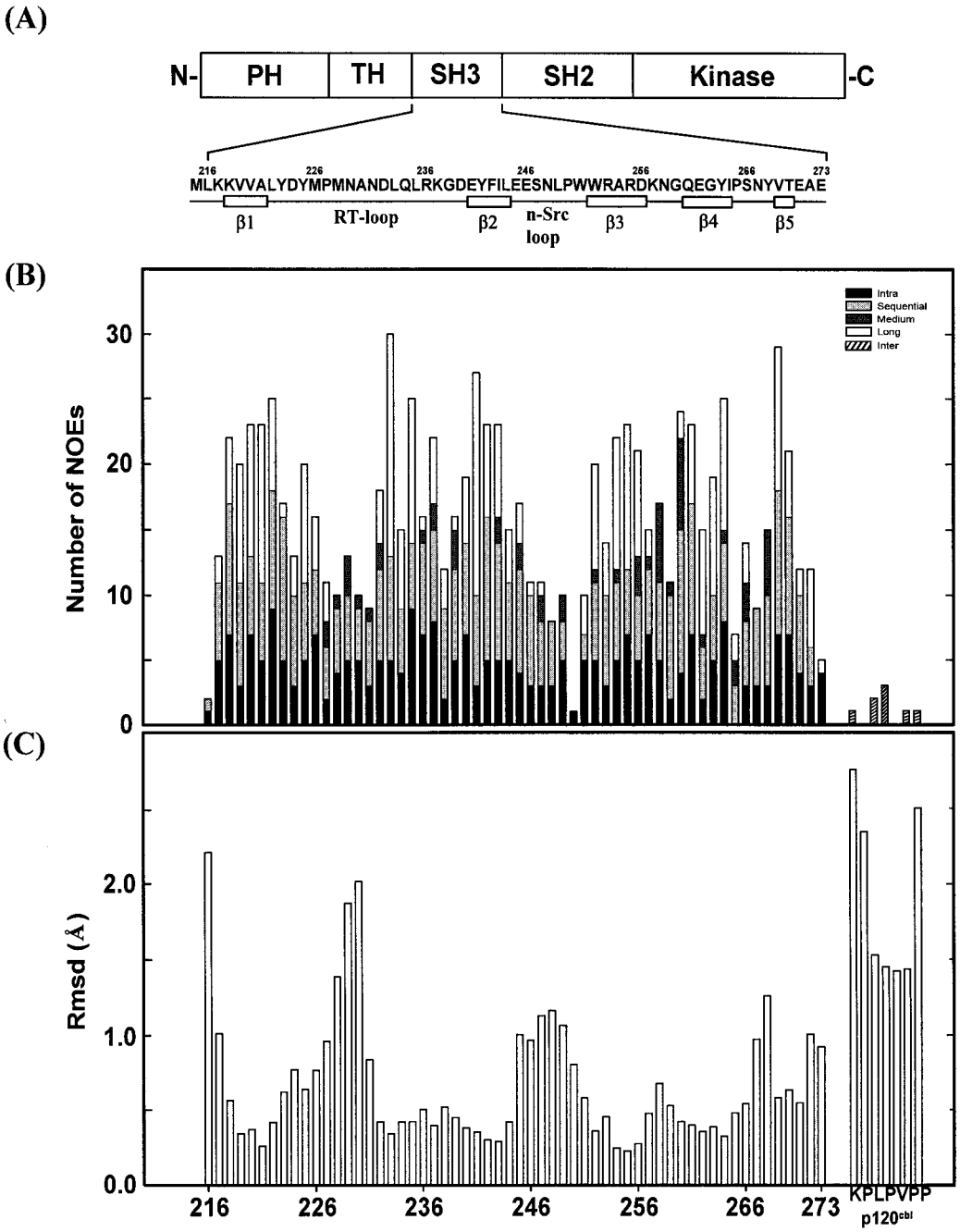

Figure 1. Summary of the sequence, experimental restraints and rmsd of the BTK SH3 domain complexed with the p120^{cbl} peptide. (A) Schematic representation of the Bruton's tyrosine kinase showing the location of SH3 domain relative to other domains. Our clone, corresponding to residues 216–273 and N-terminal Met extension, is shown. The positions of the secondary structure elements are shown under the sequence. (B) The number of ^{1}H-^{1}H NOEs per residue used as restraints in the calculation. NOEs are classified into intraresidue (black), sequential (light gray), medium (i–j < 5; dark gray), long-range (i–j ≥5; white) and intermolecular (slash). (C) Backbone rmsd for the ensemble of the final 20 structures. The rmsd values for residues 216–273 of BTK SH3 domain and residues 6–12 of the p120^{cbl} peptide are shown.

Table 1. Summary of NOE connectivities observed between BTK SH3 domain and peptide $p120^{cbl}$*

$p120^{cbl}$ peptide atoms	BTK SH3 atoms
Lys6 CγH	Trp251 C(2)H
Leu8 CγH	Trp251 N(1)H, C(7)H
Pro9 CγH	Tyr225 C(2,6)H, Tyr268 C(2,6)H
Pro9 CδH	Tyr225 C(2,6)H
Pro11 CγH, CδH	Tyr223 C(2,6)H
Pro12 CγH	Tyr268 C(2,6)H

*The sequence of the $p120^{cbl}$ peptide: SLHKDKPLPVPPYQ.

Table 2. Structure statistics for BTK-SH3/$p120^{cbl}$ peptide complex*

	<SA>	<maSA>
Rmsd from idealized geometry		
bonds (Å)	0.003 ± 0.0006	0.003
angles (deg)	0.79 ± 0.01	0.79
impropers (deg)	0.45 ± 0.01	0.45
X-PLOR energies (kcal mol^{-1})		
E_{total}	324.5 ± 6.1	300.9
E_{NOE}	55.1 ± 3.4	40.3
E_{cdih}	0.04 ± 0.01	1.7
E_{vdw}	25.4 ± 2.0	21.6
E_{bond}	13.1 ± 0.6	11.7
E_{angle}	210.7 ± 3.6	205.7
$E_{improper}$	20.2 ± 0.9	19.9

*The selected family of 20 structures was denoted <SA>, and the average structure, which was calculated by averaging superimposed coordinates, was denoted <aSA>. The <aSA> was energy minimized (and denoted <maSA>) using the same procedure as in the last refinement of the 20 structures.

cleaved from the resin by treatment with a mixture of trifluoroacetic acid and water containing phenol/1,2-ethanedithiol/thioanisole (reagent 'K'). Purification was performed on a reversed phase HPLC preparative column (Vydac, RP-18 column). The purity of the synthetic peptide was confirmed by HPLC and mass spectrometry.

NMR spectroscopy

NMR data were recorded on a Bruker Avance 600 MHz NMR spectrometer using the TPPI method. A ^{15}N-edited 3D NOESY-HSQC experiment ($\tau_m = 100$ ms) was recorded with 128 t_1 increments, 64 t_2 increments and 1024 complex data points and with water suppression using the 3-9-19 pulse sequence with gradients at 310 K. 2D ^{1}H TOCSY, NOESY ($\tau_m = 60$, 150 and 300 ms) and DQF-COSY spectra were recorded with 512 t_1 increments and 2048 complex data points at 300 and 310 K. 2D ^{15}N(ω2)-filtered NOESY (100 ms) (Ikura and Bax, 1992) and ^{15}N(ω2) half-filtered TOCSY (70 ms) (Otting et al., 1986) spectra of ^{15}N-labeled protein and unlabeled peptide (peptide:protein ratio of 4:1) were recorded with 256 t_1 increments and 2048 complex data points with spectral widths of 7500 Hz in both dimensions at 310 K. All NMR spectra were processed and analyzed on an SGI Indigo2 workstation using XWIN-NMR (Bruker).

Experimental restraints

NOE-based distance restraints were collected from analysis of 3D ^{15}N-edited NOESY-HSQC and 2D ^{1}H-NOESY spectra recorded with mixing times of 100 and 60 ms, respectively. NOEs were broadly categorized as 'strong', 'medium', and 'weak', corresponding to distance limits of 1.8–2.8, 1.8–3.5, and 1.8–5.0 Å, respectively. NOE restraints involving methyl groups and pseudoatoms were corrected by relaxing 0.3 Å to take account of equivalent atoms.

The ϕ dihedral angle was restrained to $-120 \pm 60°$ for $^3J_{HN\alpha} > 8$ Hz, and to $-120 \pm 40°$ for $^3J_{HN\alpha} > 9$ Hz. The TOCSY spectrum (15 ms), in combination with NOE intensities at short mixing time, was used to define χ^1 dihedral angle restraints. Slowly exchanging amide protons were distinguished from the 2D ^{1}H-NOESY spectrum recorded in 100% D_2O after 24 h. Hydrogen bond distance restraints were imposed for slowly exchanging NH groups for which a single hydrogen bond acceptor was identified in > 60% of structures in preliminary calculated structures. Each hydrogen bond was enforced by two distance restraints of 1.8–2.4 Å (amide proton to carbonyl oxygen) and 2.6–3.2 Å (amide nitrogen to carbonyl oxygen).

Structure calculation

The structure calculations were carried out using the Insight II 950 and X-PLOR 3.851 (Brünger, 1993) programs on an SGI Indigo 2 workstation. The starting structure of the BTK SH3 domain was generated as an extended form by using the program Insight II. The structures were calculated and refined with an ab initio simulated annealing protocol, 'sa.inp', and an SA refinement protocol, 'refine.inp', in X-PLOR 3.851. All force constants and molecular parameters, etc. were set to their default values, as in the original sa.inp and refine.inp protocols, with the exception of the timestep, which was decreased to 0.001 s through-

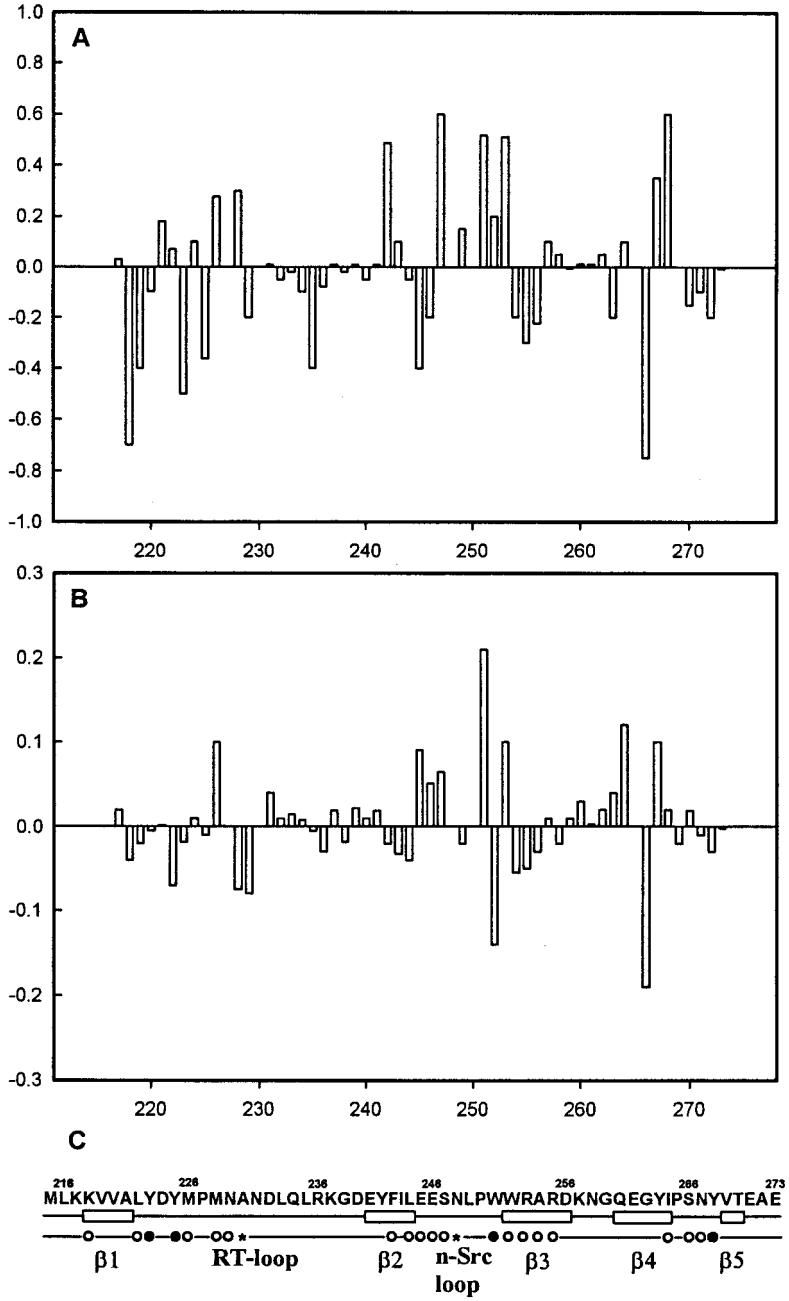

Figure 2. Chemical shift changes for (A) ^{15}N and (B) NH atoms of BTK SH3 domain upon addition of p120^{cbl} peptide to the concentration of protein/peptide = 1/4. (C) Residues of BTK SH3 domain with large chemical shift changes (^{15}N $\geq$ 0.5 ppm or NH $\geq$ 0.05 ppm) are labeled as '○', and residues involved in the intermolecular NOEs with p120^{cbl} peptide are labeled as '●'. '∗' denotes residues that were not observed in the HSQC spectrum of BTK SH3-p120^{cbl} complex.

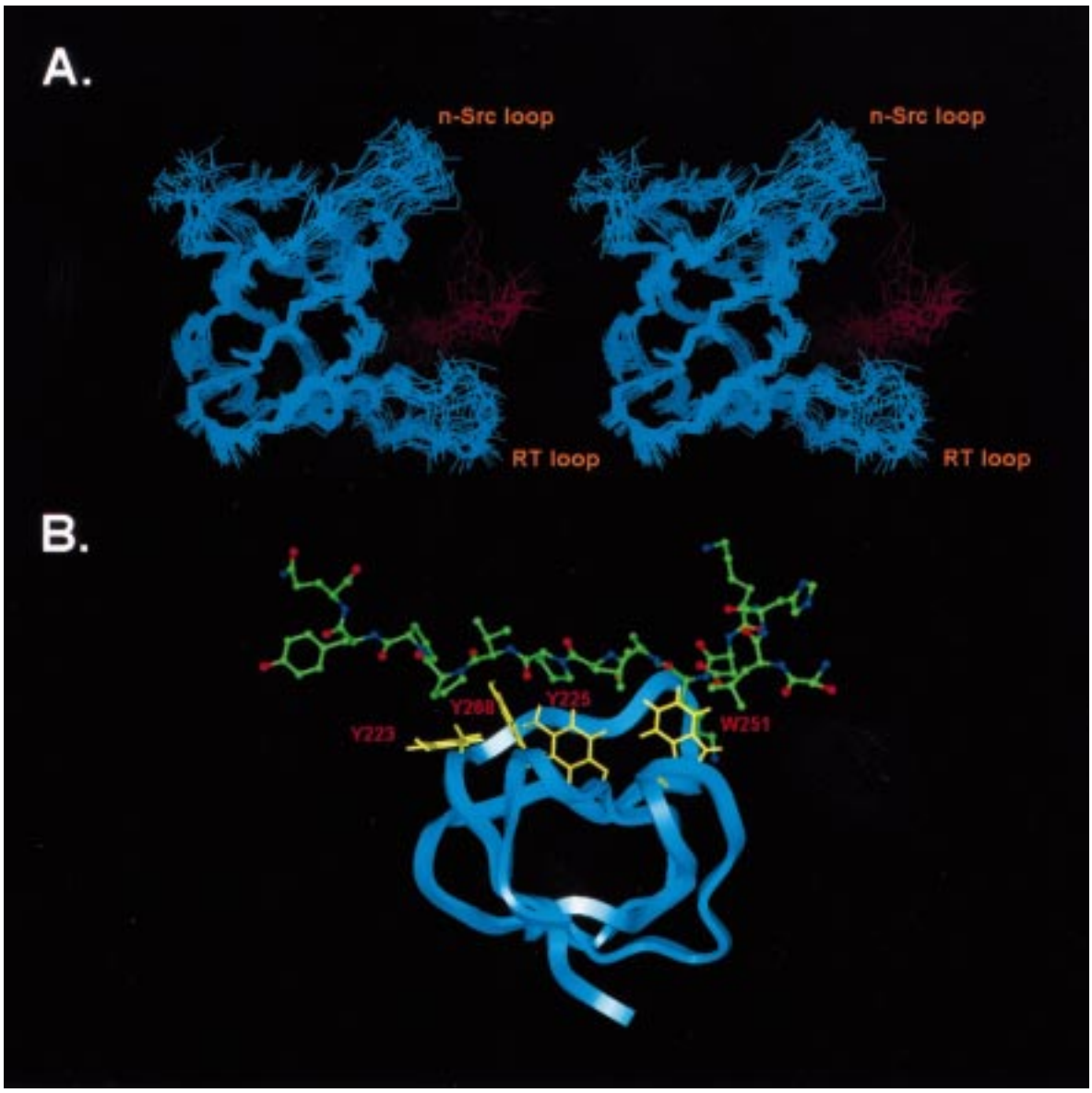

Figure 3. Solution structure of BTK SH3 domain/p120^{cbl} peptide complex. (A) A stereoview of the backbone superimposition of the final 20 structures. Residues 216–273 of the BTK SH3 domain (blue) and residues 6–12 of the p120^{cbl} peptide (red) are shown. The n-src and RT loops of the BTK SH3 domain are labeled, indicating the peptide binding regions. The structures are aligned with the average structure. (B) A schematic representation of the minimized average structure. The structure is shown as a rectangular ribbon (blue) with the four residues Y223, Y225, W251 and Y268, which exhibit NOE connectivities with the p120^{cbl} peptide shown as sticks (yellow). The p120^{cbl} peptide is shown as a ball and stick structure, colored by atom type, with the N-terminus on the right-hand side of the picture. This figure was made using the program Insight II (Molecular Simulations, San Diego, CA).

out the calculations. The final 50 structures contained no distance constraint violations greater than 0.3 Å, and dihedral angle constraint violations greater than 3°. From these structures a family of 20 was chosen based on the total energy. The representative structure was calculated by averaging the 20 structures, and this average structure was refined using the refine.inp protocol as mentioned above. The p120^{cbl} peptide was built as an extended form using the program Insight II. This peptide was then docked onto the BTK SH3 domain structure on the basis of the 9 intermolecular NOE constraints, with the BTK SH3

domain coordinates fixed. Finally, the complex was subjected to simulated annealing as described above, with the peptide ω angle kept fixed at 180° (Morton et al., 1996). A representative complex structure was calculated based on the criteria described above. The structures were displayed, analyzed and plotted with Insight II and Procheck_NMR (Laskowski et al., 1996). The coordinates of both the representative structure and the family of structures have been deposited in the Brookhaven Protein Data Bank (access number 1QLY).

Results

NMR assignments of BTK SH3 domain

The spin system identification was made primarily from 2D ^{1}H-TOCSY spectra. Sequential assignments were carried out from 100 ms 3D ^{15}N-edited NOESY-HSQC and 60 ms 2D ^{1}H-NOESY spectra using standard methods (Wüthrich, 1986). The DQF-COSY spectrum was used to determine the $^{3}J_{HN\alpha}$ coupling constants (Kim and Prestegard, 1989) and to confirm some spin system assignments. The NOEs belonging to aromatic side chains were assigned in a 60 ms 2D ^{1}H-NOESY spectrum recorded with a sample dissolved in 100% D_2O. The expressed clone covered residues 216–273 of the BTK SH3 domain, with an additional Met at the N-terminus resulting from the expression system (59 residues in total; Figure 1A). Complete assignments were obtained for the majority of the protein except two N-terminal residues of the molecule. All ^{1}H and ^{15}N chemical shift assignments in the free and complexed forms are available as Supplementary material (Table S1; to be obtained from the authors on request).

Solution structure of BTK SH3 domain/p120^{cbl} peptide complex

The p120^{cbl} peptide from the protein product of *c-cbl* protooncogene has been shown to bind with the SH3 domain of BTK and the dissociation constant (k_d) for this interaction was found to be 34.5 μM (Patel et al., 1997). Figure 2 shows a plot of the changes in chemical shifts for the backbone ^{15}N and NH atoms of BTK SH3 domain with the addition of the p120^{cbl} peptide. The residues located in the RT loop (222–229), n-Src loop (244–255) and helix-like loop between β4 and β5 (266–268) exhibited large changes in chemical shifts. The highest chemical shift changes for HN and ^{15}N atoms belong to W251 and S266, respectively.

Figure 4. Comparison of the peptide-free and peptide-bound structures of BTK SH3 domain. An overlay of the C^{α} trace of the average peptide-bound structure (yellow) with the average peptide-free structure from Hansson et al. (red) is shown using a ribbon representation. This figure was prepared using the program Insight II (Molecular Simulations, San Diego, CA).

A number of inter-molecular NOEs were identified from the 2D ^{15}N(ω2)-filtered NOESY spectrum of the BTK SH3 domain/p120^{cbl} peptide complex. The observed NOEs are summarized in Table 1. Combining the inter-molecular NOEs with chemical shift changes yields the peptide binding surface, which is similar to that observed in Fyn, Hck, Abl and Grb2 N-terminal SH3 domains complexed with proline-rich peptides (Morton et al., 1996; Wittekind et al., 1997; Horita et al., 1998; Pisabarro et al., 1998). From Table 1, inter-molecular NOEs between Lys6 and Leu8 of the p120^{cbl} peptide and the side chains of Trp251 of BTK SH3 domain define the binding orientation to be class I. Although the NOEs were insufficient to calculate a high-resolution structure of the SH3–peptide complex, the measurable constraints provide enough data to dock the peptide onto the BTK SH3 domain structure.

A total of 1059 NOE-derived distance constraints, including 368 intraresidue, 356 sequential, 56 medium ($1<i–j<5$), 270 long-range ($i–j \geq 5$) and 9 intermolecular constraints, were used in structure calculation

(Figure 1B). Backbone ϕ dihedral angles were determined for 24 residues. Stereospecific assignments of H^{β} resonances and identification of predominate χ^1 dihedral angle rotamers were made for 12 residues. Fourteen hydrogen bonds were identified as described in Materials and methods, and were added as 28 hydrogen bond distance restraints. A family of 20 structures (Figure 3A) was calculated using the procedures described in Materials and methods. The energetic and structural statistics are shown in Table 2. The rmsd calculated from the averaged coordinates for the BTK SH3 domain residues 218–271 and the $p120^{cbl}$ peptide residues 6–12 of the complex was 0.87 Å ($\pm$ 0.16 Å) for the backbone heavy atoms (N, C, and C_{α}) and 1.64 Å ($\pm$ 0.18 Å) for all heavy atoms. The rmsd value for each residue is shown in Figure 1C. Analysis of ϕ and ψ backbone angles was facilitated by using the program Procheck_NMR (Laskowski et al., 1996). There were no residues in disallowed regions and 94% of the residues were within most favored or additional allowed regions of the Ramachandran plot (Supplementary material). Three residues, N231, K237 and E271 of the BTK SH3 domain fall within generously allowed regions of the Ramachandran plot. This may be due to their locations either in more flexible regions or in the C-terminus. The topology of the BTK SH3 domain was very similar to those of other SH3 domains. Figure 3B shows the NMR-derived minimized mean structure of BTK SH3 domain complexed with the $p120^{cbl}$ peptide. Like other SH3 domains, BTK SH3 domain consists of five β-strands packed in two β-sheets forming a β-barrel-like structure and the $p120^{cbl}$ peptide binds on the BTK SH3 domain as a PPII helix in a class I orientation. Similar secondary structural elements, including the β-strands and loops, are observed in both the peptide-free structure (Hansson et al., 1998) and the peptide-bound structure determined here (Figure 4). The rmsd value between the peptide-bound and the peptide-free BTK SH3 domain (Hansson et al., 1998) was 1.34 Å for the backbone heavy atoms and 0.90 Å for the β-sheets. The similarity between the peptide-bound and peptide-free structures demonstrates that the core of the BTK SH3 domain is largely unaffected by the peptide binding and the binding sites involve mostly the side chains of the protein.

Discussion

$p120^{cbl}$ is present in early B lineage and myeloid cells. SH3 domains of numerous proteins, including Fyn, Grb2, Lck, Fgr, Nck, and PLCγ1 have been shown to bind to $p120^{cbl}$. The BTK SH3 domain binds to $p120^{cbl}$ and consequently, it is thought to be involved in signaling pathways (Cory et al., 1995). In the present study, we have determined the solution structure of BTK SH3 domain complexed with a proline-rich peptide from $p120^{cbl}$. Based on chemical shift changes and intermolecular NOEs, we have found that residues located in the RT loop, n-Src loop and helix-like loop between β4 and β5 of BTK SH3 domain are involved in ligand binding (Figures 2 and 3). We have also observed that the proline-rich peptide from $p120^{cbl}$ binds to BTK SH3 domain in a class I orientation. These results correlate well with our earlier observation that the truncated BTK SH3 domain (deletion of residues 260–273) exhibits weaker affinity for the $p120^{cbl}$ peptide (Patel et al., 1997). We have also reported earlier that the mutated SH3 domain loses its stability and structure due to deletion of 14 C-terminal aa residues (Chen et al., 1996). It is likely that the truncated SH3 domain fails to present to the ligand the crucial residues (the helix-like loop between β4 and β5 corresponding to residues 266–268) in the correct context, leading to the weaker binding.

The SH3 domain binding peptides can be divided into two groups, class I: RXXPXXP, and class II: XPXXPXR (Feng et al., 1994; Lim et al., 1994). The positioning of a basic residue (arginine or lysine) either at the beginning (class I orientation) or at the end (class II orientation) of proline-rich peptides was suggested to be the crucial determinant for the peptide orientation (Feng et al., 1994). In our present study of the $p120^{cbl}$ peptide, in which the first R is replaced by K and followed after 2 residues by the PXXP core motif, shows binding of class I. In a similar study for the specific interaction of lysine-containing proline-rich peptides with the N-terminal SH3 domain of c-Crk (Wu et al., 1995), it was observed that a lysine in the peptide is tightly coordinated by three acidic residues in the SH3 domain. In the BTK SH3/$p120^{cbl}$ peptide complex structure, although no constraint was added to restrict the side chain of K6 of the $p120^{cbl}$ peptide, the distance between N^{ϵ} of K6 and O^{δ} of D232 of the BTK SH3 domain was 4.60 Å, which is close to the distance for a potential salt bridge. Besides this, H^{β} and H^{γ} of K6 form a hydrophobic interaction with the

aromatic side chain of W251 of the BTK SH3 domain near the binding surface.

TH domain of BTK can bind to SH3 domains of Fyn, Lyn and Hck (Cheng et al., 1994; Yang et al., 1995), as it contains a proline-rich core sequence (KPLPPTP), similar to that of the $p120^{cbl}$ peptide (KPLPVPP). Previously, we have demonstrated that BTK TH domain peptide can bind to its own SH3 domain with an affinity comparable to that of binding with other SH3 domains implicated in the signaling cascade (Patel et al., 1997). In a similar study of Itk (a Tec family protein tyrosine kinase expressed in T cells), an intramolecular interaction between the proline-rich region of TH domain with its own SH3 domain was reported (Andreotti et al., 1997). Thus, BTK SH3 and TH domains may associate in a manner (i.e. class I orientation) similar to that between BTK SH3 domain and $p120^{cbl}$. This raises the possibility that BTK may associate in an inter- or intramolecular fashion to control signaling pathways. Upon inception of the signal, however, the change in BTK protein may loosen the binding of BTK SH3-TH domains. This dissociation can expose both the domains and make them available to bind to their cognate ligands. The latter process can allow further propagation of the signal. The kinase can thus make use of the strategically positioned domains to ensure timeliness, efficiency and precision in its activity. Deletion of the C-terminal 14 aa residues of SH3 domain may snap BTK of its ability to maintain its regularity and its efficiency to bind with its target. This loss of function might render the kinase abnormal.

Acknowledgements

We would like to thank Professors Shi-Han Chen (University of Washington), Shiao-Chun Tu and Ben-feng Lei (University of Houston) for their help in the protein production at the early stage of this project. We are in debt to Dr. Chinpan Chen for helpful discussions. This study was carried out on the 600 MHz NMR spectrometer at the Regional Instrument Center at Hsinchu, National Science Council, Taiwan. This work is supported by grants from the National Science Council, ROC (NSC89-2113-M-007-015) and from Dr. C.S. Tsong Memorial Medical Research Foundation (VTY88-P4-30).

References

Alexandropoulos, K., Cheng, G. and Baltimore, D. (1995) *Proc. Natl. Acad. Sci. USA*, **92**, 3110–3114.

Andreotti, A.H., Bunnell, S.C., Feng, S., Berg, L.J. and Schreiber, S.L. (1997) *Nature*, **385**, 93–97.

Brünger, A.T. (1993) *X-PLOR version 3.1: A system for X-Ray Crystallography and NMR*, Yale University Press, New Haven, CT.

Chen, Y.J., Lin, S.J., Tzeng, S.Y., Patel, H., Lyu, P.C. and Cheng, J.W. (1996) *Proteins*, **26**, 465–471.

Cheng, G., Ye, Z.S. and Baltimore, D. (1994) *Proc. Natl. Acad. Sci. USA*, **91**, 8152–8155.

Cohen, G.B., Ren, R. and Baltimore, D. (1995) *Cell*, **80**, 237–248.

Cory, G.O.C., Lovering, R.C., Hinshelwood, S., MacCarthy-Morrogh, L., Levinsky, R.J. and Kinnon, C. (1995) *J. Exp. Med.*, **182**, 611–615.

Feng, S., Chen, J.K., Yu, H., Simon, J.A. and Schreiber, S.L. (1994) *Science*, **266**, 1241–1247.

Feng, S., Kasahara, C., Rickles, R. and Schreiber, S.L. (1995) *Proc. Natl. Acad. Sci. USA*, **92**, 12408–12415.

Hammarstrom, L., Gillner, M. and Smith, C.I.E. (1993) *Curr. Opin. Immunol.*, **5**, 579–584.

Hansson, H., Mattsson, P.T., Allard, P., Haapaniemi, P., Vihinen, M., Smith, C.I. and Hard, T. (1998) *Biochemistry*, **37**, 2912–2924.

Horita, D.A., Baldisseri, D.M., Zhang, W., Altieri, A.S., Smithgall, T.E., Gmeiner, W.H. and Byrd, R.A. (1998) *J. Mol. Biol.*, **278**, 253–265.

Ikura, M. and Bax, A. (1992) *J. Am. Chem. Soc.*, **114**, 2433–2440.

Kim, Y. and Prestegard, J.H. (1989) *J. Magn. Reson.*, **84**, 9–13.

Kuriyan, J. and Cowburn, D. (1993) *Curr. Opin. Struct. Biol.*, **3**, 828–837.

Laskowski, R.A., Rullmann, J.A., MacArthur, M.W., Kaptein, R. and Thornton, J.M. (1996) *J. Biomol. NMR*, **8**, 477–486.

Lim, W.A., Richards, F.M. and Fox, R.O. (1994) *Nature*, **372**, 375–379.

Morton, C.J., Pugh, D.J., Brown, E.L., Kahmann, J.D., Renzoni, D.A. and Campbell, I.D. (1996) *Structure*, **4**, 705–714.

Otting, G., Senn, H., Wagner, G. and Wüthrich, K. (1986) *J. Magn. Reson.*, **70**, 500–505.

Patel, H.V., Tzeng, S.R., Liao, C.I., Chen, S.H. and Cheng, J.W. (1997) *Proteins*, **29**, 545–552.

Pawson, T. (1995) *Nature*, **373**, 573–580.

Pawson, T. and Schlessinger, J. (1993) *Curr. Biol.*, **3**, 434–442.

Pisabarro, M.T., Serrano, L. and Wilmanns, M. (1998) *J. Mol. Biol.*, **281**, 513–521.

Shokat, K.M. (1995) *Chem. Biol.*, **2**, 509–514.

Smith, C.I.E., Baskin, B., Humire-Grieff, P., Zhou, J.N., Olsson, P.G., Maniar, H.S., Kjellen, P., Lambris, J.D., Christensson, B. and Hammarstrom, L. (1994a) *J. Immunol.*, **152**, 557–565.

Smith, C.I.E., Islam, K.B., Vorechovsky, I., Olerup, O., Wallin, E., Rabbani, H., Baskin, B. and Hammarstrom, L. (1994b) *Immunol. Rev.*, **138**, 159–183.

Songyang, Z., Shoelson, S.E., Chaudhari, M., Gish, G., Pawson, T., Haser, W.G., King, F., Roberts, T., Ratnofsky, S., Lechleider, R.J., Neel, B.G., Birge, R.B., Fajardo, E.J., Chou, C.M., Hanafusa, H., Schaffhausen, B. and Cantley, L.C. (1993) *Cell*, **72**, 767–778.

Sparks, A.B., Rider, J.E., Hoffman, N.G., Fowlkes, D.M., Quilliam, L.A. and Kay, B.K. (1996) *Proc. Natl. Acad. Sci. USA*, **93**, 1540–1544.

Sudol, M. (1998) *Oncogene*, **17**, 1469–1474.

Tsukada, S., Saffran, D.C., Rawlings, D.J., Parolini, O., Allen, R.C., Klisak, I., Sparkes, R.S., Kubagawa, H., Mohandas, T. and Quan, S. (1993) *Cell*, **72**, 279–290.

Vetrie, D., Vorechovsky, I., Sideras, P., Holland, J., Davies, A., Flinter, F., Hammarstrom, L., Kinnon, C., Levinsky, R., Bobrow, M., Smith, C.I.E. and Bentley, D.R. (1993) *Nature*, **361**, 226–233.

Wittekind, M., Mapelli, C., Lee, V., Goldfarb, V., Friedrichs, M.S., Meyers, C.A. and Mueller, L. (1997) *J. Mol. Biol.*, **267**, 933–952.

Wu, X., Knudsen, B., Feller, S.M., Zheng, J., Sali, A., Cowburn, D., Hanafusa, H. and Kuriyan, J. (1995) *Structure*, **3**, 215–226.

Wüthrich, K. (1986) *NMR of Proteins and Nucleic Acids*, John Wiley and Sons, New York, NY.

Yang, W., Malek, S.N. and Desiderio, S. (1995) *J. Biol. Chem.*, **270**, 20832–20840.

Yu, H. and Schreiber, S.L. (1994) *Nat. Struct. Biol.*, **1**, 417–420.

Zhu, Q., Zhang, M., Rawlings, D.J., Vihinen, M., Hagemann, T., Saffran, D.C., Kwan, S.P., Nilsson, L., Smith, C.I.E., Witte, O.N., Chen, S.H. and Ochs, H.D. (1994) *J. Exp. Med.*, **180**, 461–470.